ChemPubSoc Europe

DOI: 10.1002/cmdc.201402462

CHEMMEDCHEM Full Papers

On the Metabolically Active Form of Metaglidasen: Improved Synthesis and Investigation of Its Peculiar Activity on Peroxisome Proliferator-Activated Receptors and Skeletal Muscles

Antonio Laghezza,[a] Roberta Montanari,[b] Antonio Lavecchia,[c] Luca Piemontese,[a] Giorgio Pochetti,[b] Vito Iacobazzi,[d, e] Vittoria Infantino,[d, f] Davide Capelli,[b] Michela De Bellis,[a] Antonella Liantonio,[a] Sabata Pierno,[a] Paolo Tortorella,[a] Diana Conte Camerino,[a] and Fulvio Loiodice*[a]

Metaglidasen is a fibrate-like drug reported as a selective modulator of peroxisome proliferator-activated receptor γ (PPARγ), able to lower plasma glucose levels in the absence of the side effects typically observed with thiazolidinedione antidiabetic agents in current use. Herein we report an improved synthesis of metaglidasen's metabolically active form halofenic acid (*R*)-**2** and that of its enantiomer (*S*)-**2**. The activity of the two stereoisomers was carefully examined on PPARα and PPARγ subtypes. As expected, both showed partial agonist activity toward PPARγ; the investigation of PPARα activity, however, led to unexpected results. In particular, (*S*)-**2** was found to act as a partial agonist, whereas (*R*)-**2** behaved as an antagonist. X-ray crystallographic studies with PPARγ were carried out to gain more insight on the molecular-level interactions and to propose a binding mode. Given the adverse effects provoked by fibrate drugs on skeletal muscle function, we also investigated the capacity of (*R*)-**2** and (*S*)-**2** to block conductance of the skeletal muscle membrane chloride channel. The results showed a more beneficial profile for (*R*)-**2**, the activity of which on skeletal muscle function, however, should not be overlooked in the ongoing clinical trials studying its long-term effects.

Introduction

Peroxisome proliferator-activated receptors (PPARs) are ligand-dependent transcription factors that belong to the nuclear receptor superfamily. They control the expression of genes involved in fatty acid and glucose metabolism and function as cellular lipid sensors that activate transcription in response to the binding of cognate ligands, generally fatty acids and their eicosanoid metabolites.[1–3] As ligand-dependent receptors, PPARs form heterodimers with the retinoid X receptor (RXR) and adopt an active conformation in the presence of a ligand. Additional co-regulator proteins are recruited to create a complex that binds to peroxisome proliferator response elements (PPRE) in target genes, thus regulating their expression.[4–6] There are three PPAR subtypes, commonly designated as PPARα, PPARγ, and PPARδ (β) expressed in different tissues.[7] Agonists of the γ subtype have been extensively studied for their role in regulating glucose metabolism and insulin sensitivity.[8] Full agonists of PPARγ such as rosiglitazone and pioglitazone have been developed and marketed for the treatment of type 2 diabetes.[9] However, mechanism-based side effects including weight gain, edema, congestive heart failure, and the recently reported increased risk of bone fracture following treatment with rosiglitazone or pioglitazone are major undesired effects associated with the use of PPARγ full agonists.[10,11]

As a result of the clinical observations mentioned above, emphasis has shifted to the development of partial agonists or selective PPARγ modulators (SPPARγMs). The SPPARM approach has recently attracted considerable attention because it proposes that diverse PPAR ligands, depending on their structures, would bind in a distinct manner to PPARs, inducing various levels of activation and distinct conformational changes of the receptor, leading to differential interactions with co-activa-

[a] Dr. A. Laghezza,[+] Dr. L. Piemontese, Dr. M. De Bellis, Dr. A. Liantonio, Dr. S. Pierno, Prof. P. Tortorella, Prof. D. Conte Camerino, Prof. F. Loiodice
Dipartimento di Farmacia-Scienze del Farmaco
Università degli Studi di Bari "Aldo Moro", 70126 Bari (Italy)
E-mail: fulvio.loiodice@uniba.it

[b] Dr. R. Montanari,[+] Dr. G. Pochetti, Dr. D. Capelli
Istituto di Cristallografia, Consiglio Nazionale delle Ricerche
Montelibretti, 00015 Monterotondo Stazione, Roma (Italy)

[c] Prof. A. Lavecchia
Dipartimento di Farmacia, "Drug Discovery" Laboratory
Università degli Studi di Napoli "Federico II", 80131 Napoli (Italy)

[d] Prof. V. Iacobazzi, Dr. V. Infantino
Dipartimento di Bioscienze, Biotecnologie e Biofarmaceutica
Laboratorio di Biochimica e Biologia Molecolare
Università degli Studi di Bari "Aldo Moro", 70126 Bari (Italy)

[e] Prof. V. Iacobazzi
Istituto di Biomembrane e Bioenergetica
Consiglio Nazionale delle Ricerche, 70126 Bari (Italy)

[f] Dr. V. Infantino
Dipartimento di Chimica, Università della Basilicata, 85100 Potenza (Italy)

[+] These authors contributed equally to this work.

Supporting information for this article is available on the WWW under http://dx.doi.org/10.1002/cmdc.201402462.

tors and co-repressors. Therefore, structurally diverse modulators or partial agonists are likely to elicit different pharmacological and toxicological effects depending on the context of the tissue, i.e., abundance of cofactor proteins and target gene. This may enable uncoupling of the benefits of PPAR activation from the adverse effects associated with full agonism. In agreement with the SPPARγM concept, a number of these modulators have already demonstrated desirable pharmacological profiles in various rodent models with significantly decreased side effects relative to those generally observed with existing full agonists.[12–24] One key representative is metaglidasen, a selective PPARγ partial agonist that structurally, mechanistically, and preclinically differs from the glitazones.[25] Metaglidasen is the *R* enantiomer of halofenate (**1**), a drug that was tested clinically in the 1970s as a hypolipidemic and hypouricemic agent.[26,27] Both halofenate and metaglidasen are prodrug esters that are rapidly and completely modified in vivo by nonspecific serum esterases to give the corresponding free acid form **2** (Figure 1).

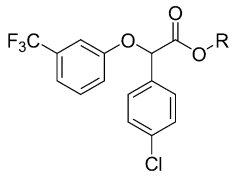

1: R = $CH_2CH_2NHCOCH_3$ (halofenate)
2: R = H (halofenic acid)

Figure 1. Structure of halofenate and its metabolically active form, halofenic acid.

Phase 2a clinical trial data indicate that metaglidasen significantly lowers plasma glucose levels in the absence of side effects such as weight gain and edema, which are observed with pharmacological agents in current use. During this development program, researchers at Metabolex discovered that metaglidasen is an effective uricosuric agent with unique properties; they repurposed the drug to treat gout with excellent safety and tolerability. Nevertheless, metaglidasen is still investigated as a useful agent for the treatment of type 2 diabetes and hyperglycemia as demonstrated by some recent patents.[28,29] Interestingly, in preclinical rodent models, metaglidasen also displays pronounced triglyceride lowering, which is often considered a hallmark of PPARα activation. However, in vivo and in vitro studies conducted with (*R*)-**1** and its metabolically active form (*R*)-**2**, respectively, indicate that this drug has no PPARα activity, suggesting that its in vivo lipid-lowering ability is therefore mediated by an alternative mechanism that has yet to be determined.[30]

Metaglidasen and halofenate show the same activity both in vitro and in vivo, suggesting a lack of stereoselectivity for PPARγ.[21,25] The mainspring for the clinical development of (*R*)-**1** in place of the more easily accessible halofenate seems to be its decreased inhibitory activity toward cytochrome P450 2C9 (CYP2C9) relative to the corresponding *dextro* isomer (*S*)-**1**.[31]

Given the promising therapeutic potential of metaglidasen, herein we describe a more convenient synthesis to obtain the active metabolite of this drug; moreover, we assign with certainty its absolute configuration, which, in a 2007 patent,[32] was attributed in a somewhat unclear manner. The transcriptional activity of the free acid form (*R*)-**2** was carefully examined with PPARα and PPARγ; the same biological evaluation was also performed on its enantiomer (*S*)-**2**, never investigated before. As expected, both stereoisomers showed partial agonist activity toward PPARγ; however, the investigation of PPARα activity led to unexpected results. In particular, (*S*)-**2** acted as a partial agonist, whereas its enantiomer behaved as an antagonist. These results were confirmed by the different effects on the PPARα-mediated gene expression of mitochondrial carnitine palmitoyltransferase 1 (CPT1), which is a molecular component of the carnitine shuttle system essential for the mitochondrial oxidation of fatty acids. X-ray crystallography on the PPARγ subtype was performed for both stereoisomers to gain greater insight into the interactions at a molecular level and to propose a binding mode that explains the lack of stereoselectivity at this receptor. Finally, because skeletal muscle is a target for PPAR agonists, the effects of both stereoisomers on the function of this tissue were evaluated by measuring the resting chloride conductance (gCl) sustained by the voltage-gated chloride channel ClC-1. Previous studies have shown that a decrease in gCl function is one of the mechanisms of action responsible for myopathies, the most significant of the complications of lipid-lowering treatment with statins and fibrates.[33–36]

Results and Discussion

Chemistry

As described in a 2007 patent, the synthesis of racemic halofenic acid **2**, the active metabolite of halofenate, is carried out in five steps.[37] The corresponding *levo* isomer, the free acid form of metaglidasen, is obtained either by the same procedure using a chiral auxiliary[32] or by resolution of the racemate.[37] The authors assigned the *R* configuration to this isomer, even though the procedure used for this attribution remains unclear. In an attempt to find a rapid and mild method to prepare (±)-halofenic acid, we applied a modified form of the procedure reported by Job, Buchwald, and co-workers,[38,39] which allowed us to obtain the target compound in a single step as shown in Scheme 1.

Racemic 4-chloromandelic acid was condensed with 1-iodo-3-trifluoromethylbenzene in the presence of a catalyst system consisting of copper(I) iodide and cesium carbonate to afford (±)-halofenic acid in 40% yield. The yield of this reaction is not remarkable, yet is fairly good considering that this procedure is

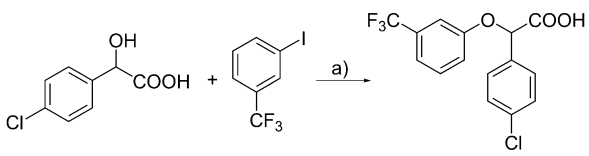

Scheme 1. Preparation of (±)-halofenic acid. *Reagents and conditions*: a) Cs_2CO_3, CuI, BuCN, 110 °C, argon, 72 h, 40% yield.

much less expensive and faster than that reported.[37] The only drawback of this reaction concerns the pH in its workup; indeed, pH values only slightly outside the range of 5–6 lead to drastic decreases in yield. The resolution of (±)-**2** was carried out by fractional crystallization from ethanol/water of the diastereomeric salts obtained with (*S*)- or (*R*)-1-(2-naphthyl)-ethylamine.[37] As an alternative to resolution, we tried to prepare (+)-**2** and (−)-**2** by the same procedure used for the racemate by starting from optically active 4-chloromandelic acid. Unfortunately, the reaction occurred with partial racemization; however, this synthetic method was useful for unambiguously assigning the absolute configuration to both isomers, given that the stereogenic center of optically active 4-chloromandelic acid was not involved in the reaction. So, starting from (*R*)-4-chloromandelic acid,[40] we obtained the partially enriched *levo* isomer of halofenic acid; this allowed us to confirm that the absolute configurations of (−)-**2** and (+)-**2** are *R* and *S*, respectively.

PPAR activity

(*R*)-**2** and (*S*)-**2** were evaluated for their agonist activity on the human PPARα (hPPARα) and PPARγ (hPPARγ) subtypes. For this purpose, GAL4–PPAR chimeric receptors were expressed in transiently transfected HepG2 cells according to a previously reported procedure.[41] The results obtained were compared with corresponding data for Wy 14,643 and rosiglitazone used as reference compounds in the PPARα and PPARγ transactivation assays, respectively. The maximum induction obtained with the reference agonist was defined as 100%.

As regards PPARγ, the transactivation assay showed this receptor to lack any stereoselectivity between (*R*)-**2** and (*S*)-**2**; in fact, both isomers acted as partial agonists with similar potency (EC_{50}: 4.8 and 7.6 μM, respectively) and efficacy (E_{max}: ~10%) confirming previously reported data[25] (Figure 2 A).

We also decided to determine the thermodynamic parameters relating to formation of the complexes of both stereoisomers with the PPARγ ligand binding domain (LBD) by isothermal titration calorimetry (ITC). ITC is a very useful alternative to conventional PPAR binding assays, which need specific radioligands for labeling of receptors. This technique, which we have successfully applied to some PPAR agonists,[42–45] measures the heat absorbed or released by titrating the protein with a ligand at constant temperature, allowing one to obtain the affinity constant. The results obtained for (*R*)-**2** and (*S*)-**2** were $1.36\times10^5\ M^{-1}$ and $1.72\times10^5\ M^{-1}$, respectively, showing that these ligands bind to PPARγ LBD with similar affinity in accordance with their functional activity. Figure 1 of the Supporting Information shows the calorimetric data (raw and integration data) obtained in the titration of PPARγ with both isomers.

Afterward we evaluated the activity of both stereoisomers toward PPARα. Previous experiments reported no activity on this receptor subtype from racemic halofenic acid and its *levo* isomer, so it was clear to assume that the *dextro* isomer was ineffective as well.[21,30] In spite of this, however, we decided to investigate the effects on PPARα of (*R*)-**2** and (*S*)-**2** because of their great similarity with some chiral α-aryloxy-α-arylacetic acids previously claimed as highly stereoselective PPARα agonists.[46] The investigation of PPARα activity led to unexpected results for the two stereoisomers. In fact, (*S*)-**2** acted as a partial agonist (EC_{50}: 11 μM, E_{max}: 31%), whereas its enantiomer behaved as an antagonist (Figure 2 B). The antagonist activity of (*R*)-**2** was confirmed by conducting a competitive binding assay in which PPARα activity at a fixed concentration of the reference agonist Wy 14,643 was measured in cells treated with increasing concentrations of (*R*)-**2**. As shown in Figure 3, (*R*)-**2** displayed a dose-dependent inhibition of Wy 14,643-mediated PPARα activity, with a half-maximal inhibitory concentration of ~21 μM. These data suggest that (*R*)-**2** is able to interact with PPARα in such a way to displace Wy 14,643 and inhibit its activity in a cellular context. It is reasonable to assume that (*R*)-**2** is able to similarly displace (*S*)-**2**, thus explaining why racemic halofenic acid does not display PPARα activity.

To further corroborate the differing results between (*R*)-**2** and (*S*)-**2** on PPARα activity, we investigated the effects of both stereoisomers on mitochondrial carnitine/acylcarnitine carrier (CAC) and carnitine palmitoyltransferase 1 (CPT1) PPARα-mediated gene expression. These two molecular components of the

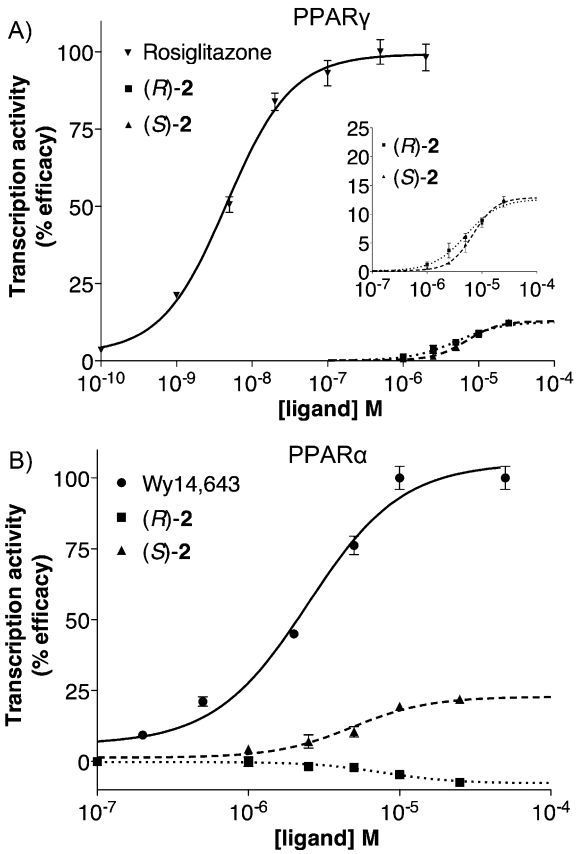

Figure 2. Gal4 reporter assay data for A) human PPARγ and B) human PPARα. A Gal4–hPPARγ or Gal4–hPPARα ligand binding domain expression plasmid was co-transfected with a luciferase reporter plasmid in HepG2 cells. The insert in panel A) is a magnification of the curves that relate only to compounds (*R*)-**2** and (*S*)-**2**. Data are normalized with respect to control, and values are the mean ± SEM of $n = 3$ experiments performed in duplicate.

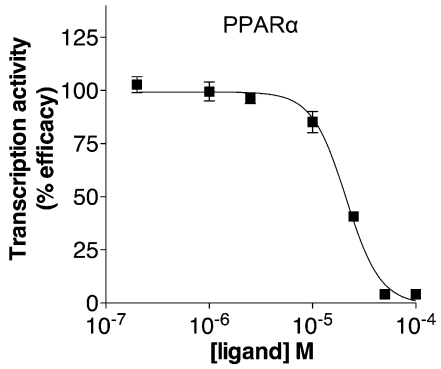

Figure 3. PPARα antagonist effect of (*R*)-**2**. PPARα activity was measured in Gal4–hPPARα LBD transfected cells treated with Wy 14,643 at 10 μM and increasing concentrations of (*R*)-**2**. Data are normalized with respect to control, and values are the mean ± SEM of $n = 2$ experiments performed in triplicate.

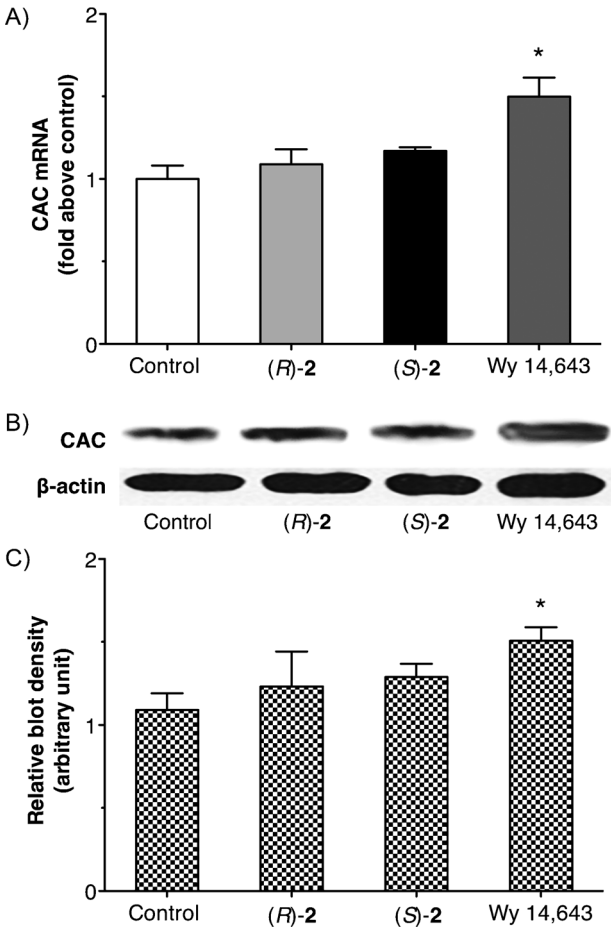

Figure 4. A) Total RNA extracted from HepG2 cells, treated with or without 50 μM (*R*)-**2**, 50 μM (*S*)-**2**, or 50 μM Wy 14,643 for 24 h, was used to quantify CAC mRNA by real-time PCR; data are the mean ± SD of three independent duplicate experiments. B) CAC and β-actin of HepG2 cells, treated for 48 h as described for panel A), were immunolabeled with specific antibodies. C) The intensities of immunolabeled protein bands depicted in panel B) were quantified by densitometric scanning. Quantitation represents fold change of CAC protein signals relative to control cells; data are the mean ± SD from three independent experiments (*$p < 0.05$; one-way ANOVA, Bonferroni test).

carnitine shuttle system are essential for the mitochondrial oxidation of fatty acids, because they catalyze the entry of fatty acid acyl groups into the mitochondrial matrix, where the enzymes of fatty acid β-oxidation are located. Recent studies demonstrated that transcription of the CAC gene is enhanced by statins and fibrates, providing a novel contribution to the understanding of their hypolipidemic action.[42,47,48] Therefore, we decided to test (*S*)-**2** and (*R*)-**2** with the aim to determine if these fibrate-like drugs are able to similarly up-regulate mitochondrial CAC and CPT1 gene expression. The effects of in vitro application of these compounds were investigated on HepG2 cells, which were incubated for 48 h with (*S*)-**2** and (*R*)-**2** at 50 μM. The PPARα agonist Wy 14,643 (50 μM) was used as a reference compound. After incubation, total mRNA was extracted and used to determine CAC and CPT1 transcript levels. As shown in Figures 4A and 5A, (*R*)-**2** did not induce any increase of CAC and CPT1 mRNA, as expected; in contrast, (*S*)-**2** caused a ~1.5-fold increase in CPT1 mRNA, whereas no effect was detected for CAC mRNA. Consistently, western blotting analysis showed no effects on CAC and CPT1 protein levels from (*R*)-**2** (Figure 4B,C and 5B,C) whereas it confirmed a significant, albeit weak, increase in CPT1 protein level (Figure 5B,C) in cells treated with (*S*)-**2**. The observed effects of (*S*)-**2** on CPT1 gene expression level, however, turned out to be lower than that obtained with Wy 14,643 at the same concentration.

Given that no crystal structures of PPARα complexed with carboxylic antagonists are available as a starting point for docking, X-ray crystal studies of the complexes PPARα–(*S*)-**2** and PPARα–(*R*)-**2** will be crucial to confirm the obtained results. These studies are still in progress for PPARα, whereas they have already been achieved for PPARγ with the aim to provide a molecular explanation for the lack of stereoselectivity of this receptor toward (*R*)-**2** and (*S*)-**2**.

Binding of (*R*)-2 in the PPARγ LBD

The final omit map (Figure 6A) showed clear electron density where one molecule of (*R*)-**2** can be easily fitted. This isomer was accommodated between helix 3 and the β-sheet, where one of its carboxylic oxygen atoms was found to form a hydrogen bond (2.7 Å) with the NH group of S342 belonging to the β-sheet (Figure 7A). This interaction has often been observed in other PPARγ complexes with partial agonists. Upon binding, the ligand forced the side chains of R288 and E291 to assume different conformations. In this new orientation, the charged guanidinium group of R288 interacts with the electronegative trifluoromethyl group of the ligand (3.5 Å) and made van der Waals (vdW) interactions with the residue A292 belonging to helix 3. The chlorine atom, at the opposite extremity of the ligand, is directed toward a hydrophobic core of the LBD formed by the side chains of I281, L353, F363, and M364 (Figure S2, Supporting Information). The shortest distances of the chlorine atom were with one methyl group of I281 (3.7 Å) and a carbon atom of the aromatic ring of F363 (3.7 Å). A LigPlot analysis[49] of the vdW interactions of (*R*)-**2** is shown in Figure S3A in the Supporting Information.

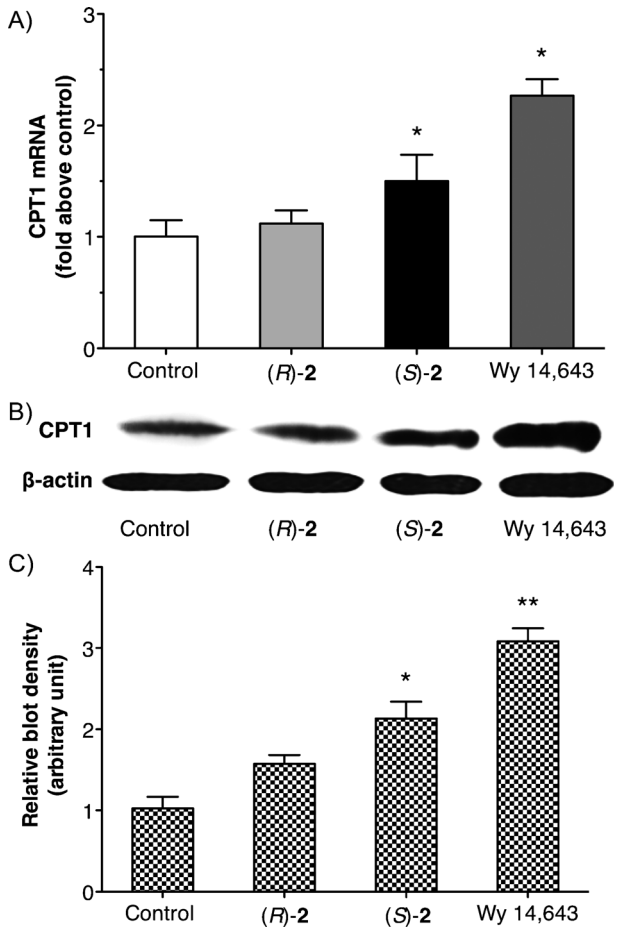

Figure 5. A) Total RNA extracted from HepG2 cells, treated with or without 50 μM (*R*)-**2**, 50 μM (*S*)-**2**, or 50 μM Wy 14,643 for 24 h, was used to quantify CPT1 mRNA by real-time PCR; data are the mean ± SD of three independent duplicate experiments. B) CPT1 and β-actin of HepG2 cells, treated for 48 h as described for panel A), were immunolabeled with specific antibodies. C) The intensities of immunolabeled protein bands depicted in panel B) were quantified by densitometric scanning. Quantitation represents fold change of CPT1 protein signals relative to control cells; data are the mean ± SD from three independent experiments (*$p < 0.01$, **$p < 0.001$; one-way ANOVA, Bonferroni test).

Binding of (*S*)-2 in the PPARγ LBD

Enantiomer (*S*)-**2** also bound to PPARγ assuming the typical position of partial agonists, although more shifted toward the entrance of the LBD (Figure S4, Supporting Information). (*S*)-**2** faced the β-sheet and both its carboxylic oxygens were found to be engaged in two hydrogen bonds with the NH group of S342 and the side chain OH of S342, respectively (Figure 7B). The side chain of R288 maintained its typical position (*t* conformation), and its guanidinium group made two hydrogen bonds with one of the ligand carboxylic oxygen atoms and the NH group of E343, respectively. The ligand electronegative CF_3 group interacted with the positively charged side chain of R288 through a water molecule also bridged with the CO of L340 (Figure 7B). One of the fluorine atoms also contacted the residue C285 at distances of ~3.0 Å. (*S*)-**2** formed more and stronger interactions than (*R*)-**2** with H3 and the β-sheet, better stabilizing these regions of the LBD (Figure S3B, Supporting Information). The largest number of hydrogen bonds and vdW interactions realized by this ligand, in comparison with (*R*)-**2**, was in accordance with the more favorable enthalpic contribution observed in the ITC experiment upon binding to PPARγ LBD (−6.5 vs. −3.8 kcal mol^{-1}, respectively). The omit map around (*S*)-**2** is shown in Figure 6B.

Superimposition of (*R*)-**2** and (*S*)-**2** in the PPARγ LBD (Figure 8A) shows that the two enantiomers, although both interacting with the NH group of S342 through their carboxylic oxygen atoms, occupy slightly different positions between H3 and the β-sheet, with the *S* enantiomer less inserted into the LBD cavity. The superimposition with other known PPARγ partial agonists showed that (*R*)-**2** occupied the same position of **3** (MRL24)[50] (PDB code 2Q5P) and (*S*)-**2**, that of the partial agonist **4** (FS214)[42] (PDB code 4E4Q) (Figure 8B,C). Both stereoisomers seem to be able to stabilize, even though in different ways, the same region of the receptor (H3 and β-sheet), thus explaining their similar affinity and activity toward PPARγ.

The binding mode of (*R*)-**2** would also explain its ability to inhibit the CDK5-mediated phosphorylation of PPARγ. Recently, in fact, Choi et al. reported this biochemical effect at the level of S273 of PPARγ2 (corresponding to S245 of PPARγ1) for rosiglitazone and some PPARγ partial agonists including (*R*)-**1**.[50] This study suggests that both thiazolidinediones (TZDs) and partial agonists with antidiabetic effects improve insulin sensitivity primarily by this mechanism. Inhibition of S273 phosphorylation seems to be distinct from classical transcriptional activation, which involves the stabilization of the highly dynamic activation of helix 12 and appears to mediate at least some of the undesirable side effects of chronic PPARγ activation. In this study, using amide hydrogen/deuterium exchange kinetics, the authors showed that binding of the PPARγ partial agonist **3** significantly decreases flexibility of the loop region around S273 and that both rosiglitazone and **3** decrease the mobility of helix 3 and the adjacent β-sheet, which are sites for potential interaction with co-reg-

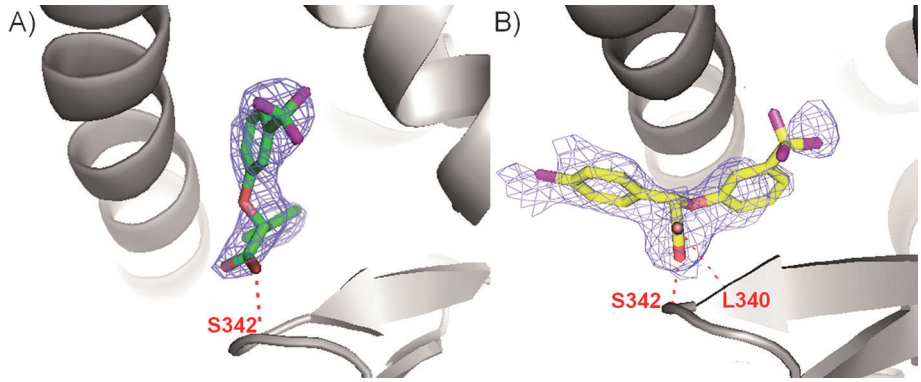

Figure 6. 2F_o−F_c omit map calculated around A) (*R*)-**2** (green) and B) (*S*)-**2** (yellow) in complex with PPARγ.

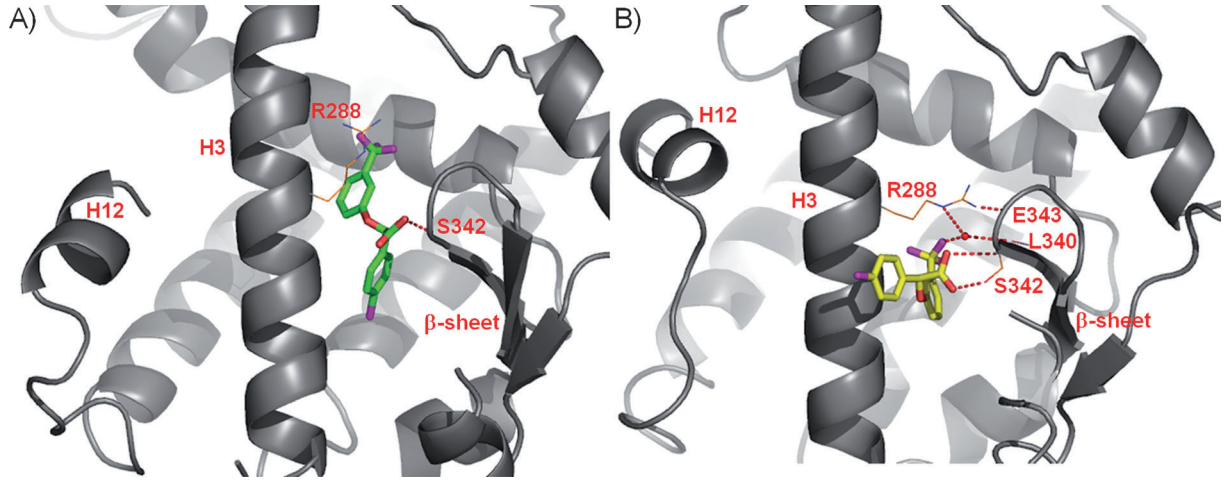

Figure 7. Hydrogen bond network of A) (*R*)-**2** (green) and B) (*S*)-**2** (yellow) in complex with PPARγ.

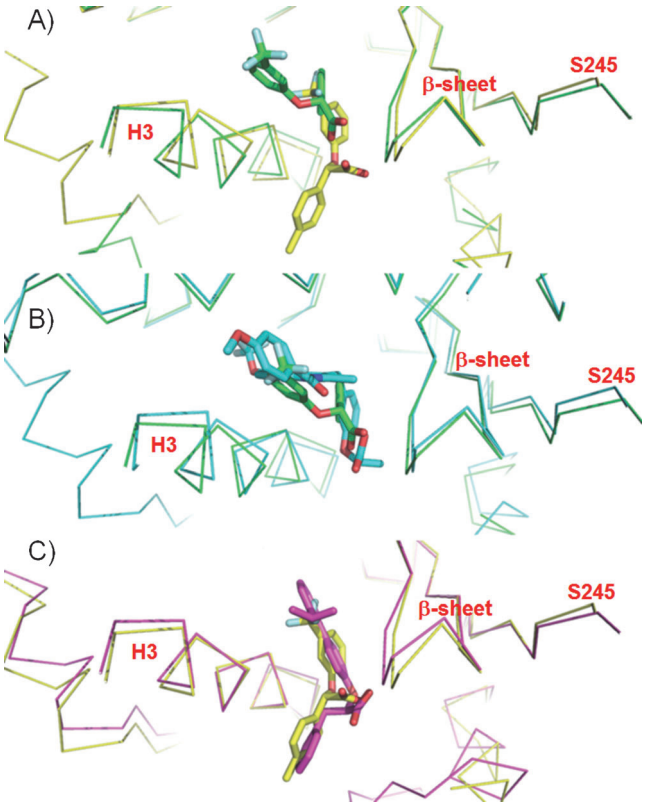

Figure 8. Superpositions of A) (*R*)-**2** (green) and (*S*)-**2** (yellow); B) (*R*)-**2** (green) and **3** (cyan); C) (*S*)-**2** (yellow) and **4** (magenta) into the LBD of PPARγ1. S245 of PPARγ1 corresponds to S273 of PPARγ2.

ulatory proteins. These findings suggest that ligand-induced decreases in the dynamic nature of helix 3, the β-sheet, and the CDK5 site, may "freeze" this region into a conformation less favorable to CDK5-mediated phosphorylation. According to this hypothesis, it is likely that (*R*)-**2** decreases the dynamics of helix 3, β-sheet, and CDK5 site, explaining the consequent decrease of PPARγ phosphorylation at S273. This could be the principal molecular mechanism responsible for its antidiabetic activity and lack of undesirable side effects typical of classical PPARγ full agonists. A similar behavior could also be suggested for (*S*)-**2**, which binds to the same region of PPARγ LBD, although slightly shifted with respect to (*R*)-**2**.

Effects of (*R*)-2 and (*S*)-2 on skeletal muscle chloride conductance

Statins and PPAR agonists such as fibrates are widely used in therapy to treat hyperlipidemia. However, clinical evidence has shown drug-associated skeletal muscle disorders ranging from myalgia to severe myopathy.[35] This type of myopathy has been characterized biochemically and morphologically, and there are a few mechanistic hypotheses.[35] Our previous studies allowed us to identify the target of the skeletal muscle damage; in fact, both statins and fenofibrate are able to reduce resting chloride conductance (gCl), sustained by the voltage-gated chloride channel ClC-1, a parameter that controls sarcolemma electrical stability and functional processes such as excitation and contraction. A reduced gCl causes disorders related to abnormal action potential firing.[36,51] On this basis, we decided to test (*R*)-**2** and (*S*)-**2** to assess the possibility that these fibrate-like drugs were able to interfere with the chloride ion flux of skeletal muscle membrane, as previously reported for similar compounds.[36,51,52]

The effects of in vitro application of these compounds were evaluated on extensor digitorum longus (EDL) muscle in terms of resting membrane ionic conductances and excitability parameters. As can be seen in Figure 9, both enantiomers significantly decreased gCl in a concentration-dependent manner, with (*S*)-**2** more potent than (*R*)-**2**. In particular, the application of (*S*)-**2** produced a significant ($p < 0.001$, Student's *t* test) 32 and 43% block of gCl at 10 and 100 μM, respectively, relative to the control value. (*R*)-**2**, instead, produced a lower, although significant ($p < 0.01$, Student's *t* test), decrease in gCl by 11 and 30% at 10 and 100 μM, respectively. The resting potassium conductance (gK) was slightly and not significantly increased from 366 ± 61 to 435 ± 35 μS cm^{-2} when a 100 μM dose of the less potent *R* enantiomer was applied to the muscle bath solution. The effects of the two enantiomers were completely reversible,

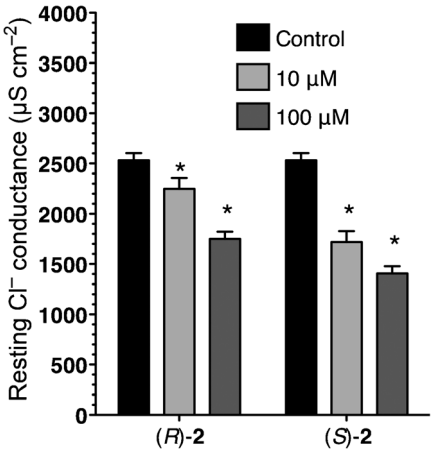

Figure 9. Resting gCl measured in EDL muscle before and after in vitro application of either (*R*)-**2** or (*S*)-**2**. Data represent the mean ± SEM from 17–49 fibers (*$p < 0.01$, Student's *t* test).

because after the application of the normal solution, the gCl value was similar to that recorded in the absence of drugs.

We also measured the excitability parameters of EDL muscle fibers upon exposure to (*R*)-**2** at 100 μM (Figure 10). Concurrently with the decrease in gCl we found an increase in membrane excitability. Interestingly, we observed a significant decrease (15%) of the current (Ith) required to elicit the first action potential (AP) together with a significant twofold increase in the action potential latency (Lat) ($p < 0.01$). However, no significant differences were observed in the amplitude of the AP and the maximum number (*N*) of spikes (data not shown).

At this point, given that intracellular calcium homeostasis is a critical determinant of muscle function,[53] in order to evaluate the potential ability of the drug to induce muscle damage by interfering with Ca^{2+} signaling machinery, we decided to evaluate the effects of (*R*)-**2** and (*S*)-**2** on calcium homeostasis of native rat skeletal muscle fibers. These effects were evaluated by fura-2 microspectrofluorimetric analysis. Both drugs, tested in a concentration range of 10–100 μM, did not produce any change in resting cytosolic calcium. Particularly, the ratio value (I_{340}/I_{380}) was 0.31 ± 0.004 ($n = 16$) and 0.29 ± 0.004 ($n = 15$) in the absence and presence of 100 μM (*R*)-**2**, respectively; similar results, respectively 0.30 ± 0.005 ($n = 15$) and 0.29 ± 0.008 ($n = 14$), were obtained in the absence and presence of (*S*)-**2** at 100 μM. Both compounds, therefore, did not interfere with calcium homeostasis, thus indicating a lack of potential toxicity at this level. Because intracellular calcium levels can affect muscle gCl through modulation of the calcium-dependent protein kinase C,[54] these results allow us to hypothesize that the decrease in gCl induced by both molecules is likely due to direct inhibition of the ClC-1 chloride channel.

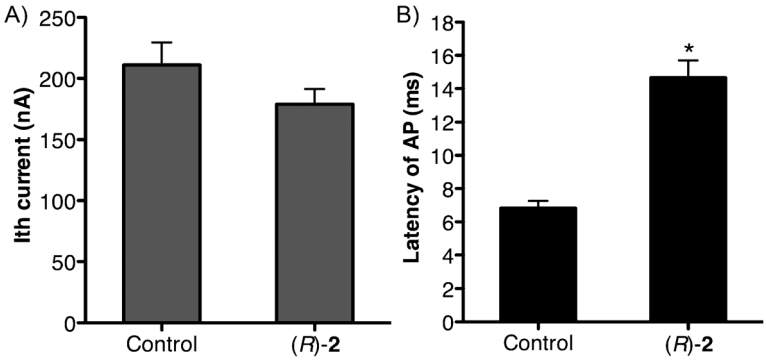

Figure 10. Excitability parameters measured in EDL muscle after in vitro application of (*R*)-**2** (100 μM). A) The current (Ith) required to induce the first action potential (AP) was decreased by 15%, and B) the latency to obtain the AP was significantly increased with respect to control. Data represent the mean ± SEM from 10–19 fibers (*$p < 0.01$, Student's *t* test).

Conclusions

In the present study we report an improved synthesis of the metabolically active form (*R*)-**2** of metaglidasen, a selective PPARγ modulator, which, even though repurposed as a drug to treat gout due to its unique uricosuric properties, is still investigated as a useful agent for the treatment of type 2 diabetes and hyperglycemia. Its activity and that of its enantiomer on both PPARα and PPARγ were carefully investigated. As previously reported, they showed similar activity at PPARγ; therefore, with the aim to provide a molecular explanation for this unusual lack of stereoselectivity, X-ray crystallography studies with the PPARγ LBD were performed for both enantiomers. Both (*R*)-**2** and (*S*)-**2** bound to the same region of the LBD, although slightly shifted with respect to each other, contributing to a reduction in the dynamics of H3, β-sheet, and CDK5 site. Interestingly, this binding mode seems to be common to all effective antidiabetic PPARγ ligands able to inhibit CDK5-mediated phosphorylation of S273, a mechanism that is suggested to be responsible, at least in part, for the improved insulin sensitivity by these drugs.

In contrast, unexpected results were obtained at PPARα. In this case, (*S*)-**2** exhibited a partial agonist activity, whereas (*R*)-**2** displayed an antagonism profile. These results were confirmed by the different effects on the PPARα-mediated gene expression of mitochondrial carnitine palmitoyltransferase 1 (CPT1), which is a molecular component of the carnitine shuttle system essential for the mitochondrial oxidation of fatty acids. Given that no crystal structures of PPARα complexed with carboxylic antagonists are available as a starting point for docking analysis, X-ray structure determination of the crystal complexes involving PPARα and each of the two stereoisomers will be crucial to confirm the obtained results. These studies are still in progress for PPARα.

Finally, we evaluated the blocking activity of both (*R*)-**2** and (*S*)-**2** on skeletal muscle chloride conductance, which is related to myopathies frequently observed in treatment with lipid-lowering drugs. The results showed a more beneficial profile

for (*R*)-**2**; nevertheless, the activity of this isomer on skeletal muscle function should not be overlooked in the current clinical trials, especially when studying the long-term effects.

In conclusion, it appears that a more careful investigation of the structural determinants of the metabolically active form of metaglidasen could allow the identification of new analogues with improved pharmacological properties, that is, a dual PPARα/γ activity associated with low inhibition of cytochrome P450 and decreased blocking activity on skeletal muscle chloride conductance. In this perspective, particular attention must be paid to the stereochemistry, which, as widely reported for PPAR ligands, plays a key role in the biological activity of these compounds.

Experimental Section

Chemistry

Melting points were determined in open capillaries on a Gallenkamp electrothermal apparatus and are uncorrected. Mass spectrometric data were recorded on an HP GC–MS 6890–5973 MSD spectrometer, electron impact 70 eV, equipped with HP chemstation. ^{1}H NMR spectra were recorded in $CDCl_3$ on a Varian Mercury 300 (300 MHz) spectrometer at room temperature. Chemical shifts (δ) are expressed as parts per million. The purity of all tested compounds was $>95\%$, as confirmed by combustion analysis carried out with an Eurovector Euro EA 3000 model analyzer. Optical rotations were measured with a PerkinElmer 341 polarimeter at room temperature (20 °C): concentrations are expressed as g(100 mL)$^{-1}$. The enantiomeric excesses of the final compounds were determined by HPLC analysis on Chiralcel AD or OD column (4.6 mm i.d.×250 mm, Daicel Chemical Industries Ltd., Tokyo, Japan). Analytical liquid chromatography was performed on a PE chromatograph equipped with a Rheodyne 7725i model injector, a 785A model UV/Vis detector, a series 200 model pump and an NCI 900 model interface. Chemicals were from Aldrich (Milan, Italy) and Alfa Aesar (Karlsruhe, Germany) and were used without further purification.

Synthesis of (*R*,*S*)-2-(4-chlorophenyl)-2-(3-trifluoromethyl)phenoxyacetic acid [(*R*,*S*)-2]. 1-Iodo-3-trifluoromethylbenzene (1.3 mmol), cesium carbonate (2 mmol) and copper(I) iodide (0.05 mmol) were added to a solution of (*R*,*S*)-4-chloromandelic acid (1 mmol) in butyronitrile (2 mL) under argon atmosphere. The resulting mixture was stirred at 110 °C for 72 h. Then the solvent was distilled off and the solid was poured into water and washed twice with ethyl acetate. The aqueous phase was acidified up to pH 5–6 with 10% citric acid and extracted (3×10 mL) with ethyl acetate. The organic layer was washed with brine, dried over Na_2SO_4 and filtered. The solvent was evaporated to dryness to afford a solid that was crystallized from *n*-hexane. The title compound was obtained as a white solid in 40% yield; mp: 99–100 °C; GC–MS, (methyl ester) *m/z* (%) = 346 (1) [$M^+ + 2$], 344 (2) [M^+], 285 (25), 183 (100), 155 (83); ^{1}H NMR: $\delta = 7.04$–7.54 (9H, m, 8 aromatics + COOH, D_2O exchanged), 5.65 ppm (1H, s, CH).

Resolution of (*R*,*S*)-2. The racemate (1 mmol) was poured into a boiling mixture of water (3.5 mL) and 96% ethanol (5 mL) together with (*S*)-1-(2-naphthyl)ethylamine (0.5 mmol) and KOH (0.5 mmol). The solution was cooled to room temperature; after 12 h the resulting crystals were collected by filtration and recrystallized using a mixture of water (1.75 mL) and ethanol 96° (3.75 mL). The so obtained crystalline diastereomeric salt was suspended in diethyl ether and washed with 2 N HCl and brine. The organic layer was dried over Na_2SO_4 and filtered. The solvent was distilled off to afford a white solid that was crystallized from *n*-hexane to give (*R*)-2-(4-chlorophenyl)-2-(3-trifluoromethyl)phenoxyacetic acid in 59% yield (0.30 mmol). The mother liquors obtained from the first crystallization of the diastereomeric salts were evaporated to dryness and the residue was suspended in diethyl ether and washed with 2 N HCl and brine. The organic layer was dried over Na_2SO_4, filtered and evaporated to dryness. The white residue (0.4 mmol) was poured into a boiling mixture of water (1.4 mL) and 96% ethanol (2 mL) together with (*R*)-1-(2-naphthyl)ethylamine (0.2 mmol) and KOH (0.2 mmol). The solution was cooled to room temperature; after 12 h the resulting crystals were collected by filtration and treated as described above to afford a white solid that was crystallized from *n*-hexane to give (*S*)-2-(4-chlorophenyl)-2-(3-trifluoromethyl)phenoxyacetic acid in 67% yield (0.34 mmol).

(*S*)-2: mp: 98–99 °C; $[\alpha]_D = +91$ ($c = 0.1$, MeOH); *ee* = 99% (methyl ester, Chiralcel OD column, *n*-hexane/*i*PrOH 95:5 as a mobile phase, flow rate: 0.5 mL min^{-1}, detection: 254 nm; $t_R = 10.2$ min); Anal. calcd for $C_{15}H_{10}ClO_3F_3$: C 54.48, H 3.05, found: C 54.55, H 3.31.

(*R*)-2: mp: 99–100 °C; $[\alpha]_D = -90.5$ ($c = 0.1$, MeOH); *ee* = 98% (methyl ester, Chiralcel OD column, *n*-hexane/*i*PrOH 95:5 as a mobile phase, flow rate: 0.5 mL min^{-1}, detection: 254 nm; $t_R =$ 11,4 min); Anal. calcd for $C_{15}H_{10}ClO_3F_3$: C 54.48, H 3.05, found: C 54.35, H 3.11.

Resolution of 4-chloromandelic acid. (*R*)-4-Chloromandelic acid was obtained as reported.[40] Briefly, (*R*)-1-phenylethylamine (2.0 g, 16.5 mmol) was added to a solution of racemic 4-chloromandelic acid (3.0 g, 16.1 mmol) in 20 mL of 95% ethanol. The resulting mixture was held at reflux for 15 min and then slowly cooled to room temperature. A crystalline salt (2.4 g) with $[\alpha]_D = -33$ ($c = 1.0$, EtOH) was collected by filtration and recrystallized from 95% ethanol (15 mL). The salt obtained (1.8 g), having $[\alpha]_D = -44$ ($c = 1.0$, EtOH), was recrystallized again from 95% ethanol (10 mL) to give the (*R*,*R*) diastereomeric salt (1.0 g) with $[\alpha]_D = -49$ ($c = 1.0$, EtOH). This salt was treated with 2 N HCl and extracted (3×75 mL) with diethyl ether. The organic phase was washed with brine, dried over Na_2SO_4 and filtered. The solvent was evaporated to dryness to afford (*R*)-4-chloromandelic acid as a white solid (0.6 g). (*S*)-4-Chloromandelic acid was obtained in the same manner starting from racemic 4-chloromandelic acid and (*S*)-1-phenylethylamine. GC–MS, (methyl ester) *m/z* (%) = 202 (3) [$M^+ + 2$], 200 (10) [M^+], 141 (100), 77 (72); ^{1}H NMR: $\delta = 7.33$–7.40 (4H, m, aromatics), 5.21 (1H, s, CH), 4.67 ppm (2H, b, OH + COOH, D_2O exchanged).

(*S*)-4-Chloromandelic acid. $[\alpha]_D = +135$ ($c = 1.0$, MeOH); *ee* = 99% (methyl ester, Chiralcel AD column, *n*-hexane/*i*PrOH 95:5 as a mobile phase, flow rate: 0.5 mL min^{-1}, detection: 254 nm; $t_R =$ 16,5 min).

(*R*)-4-Chloromandelic acid. $[\alpha]_D = -135$ ($c = 1.0$, MeOH); *ee* = 99% (methyl ester, Chiralcel AD column, *n*-hexane/*i*PrOH 95:5 as a mobile phase, flow rate: 0.5 mL min^{-1}, detection: 254 nm; $t_R =$ 17,8 min).

Synthesis of partially enriched (*S*)-2 and (*R*)-2. These compounds were synthesized by using the method described above for (*R*,*S*)-**2**, but starting from (*S*)- and (*R*)-4-chloromandelic acids, respectively. The reaction was carried out at 75 °C instead of 110 °C.

(*S*)-2: mp: 99–100 °C; $[\alpha]_D = +45$ ($c = 0.1$, MeOH); *ee* = 77% (methyl ester, Chiralcel OD column, *n*-hexane/*i*PrOH 95:5 as a mobile phase, flow rate: 0.5 mL min^{-1}, detection: 254 nm; $t_R = 10{,}2$ min).

(*R*)-**2**: mp: 98–100 °C; $[\alpha]_D = -16$ ($c = 0.1$, MeOH); *ee* = 30% (methyl ester, Chiralcel OD column, *n*-hexane/*i*PrOH 95:5 as a mobile phase, flow rate: 0.5 mL min^{-1}, detection: 254 nm; $t_R = 11{,}4$ min).

Protein expression, purification and crystallization

The LBD of PPARγ was expressed in BL21 DE3 cells as N-terminal His-tagged protein using a peT28 vector. The protein was purified onto a Ni^{2+}-nitriloacetic acid column (GE Healthcare) as previously described.[55] Crystals of apo-PPARγ were obtained by the vapor diffusion method at 18 °C using a sitting drop made by mixing 2 μL of protein solution (10 mg mL^{-1}, in 20 mM Tris, pH 8.0, 1 mM TCEP and 0.5 mM EDTA) with 2 μL of reservoir solution (0.8 M sodium citrate and 0.15 M Tris, pH 8.0). Crystals were soaked for two weeks in a storage solution (1.2 M sodium citrate and 0.15 M Tris, pH 8.0) containing the ligand (0.25 mM). The ligand was dissolved in DMSO and added to the storage solution so that the final concentration of DMSO was 0.5%. The storage solution with glycerol [20% (*v*/*v*)] was used as a cryoprotectant. Crystals belong to the space group *C*2 with cell parameters shown in Table S1, Supporting Information.

Structure determination

X-ray crystallographic data were collected at 100 K under a nitrogen stream using synchrotron radiation (beamline ID29 at ESRF, Grenoble, France). The diffracted intensities were processed using the programs MOSFLM and SCALA.[56] Structure solution was performed with AMoRe,[57] using the coordinates of PPARγ/(*S*)-2-(4-phenylphenoxy)-3-phenylpropanoic acid (LT175; PDB code 3B3K) as the starting model. The coordinates were then refined with the Phenix 1.8.4 package.[58] All data between 58 and 2.6 Å were included for both structures. The statistics of crystallographic data and refinement are summarized in Table S1, Supporting Information. The coordinates of PPARγ/(*R*)-**2** and PPARγ/(*S*)-**2** have been deposited in the Brookhaven Protein Data Bank (PDB) with access codes 4PVU and 4PWL, respectively.

Isothermal titration calorimetry

ITC experiments were performed at 25 °C using a MicroCal ITC200 microcalorimeter (MicroCal Inc., Northampton, MA, USA) as previously described.[42] Briefly, the protein solution (50 μM) was placed in the sample cell, and the ligand solution (500 μM) was loaded into the syringe injector. The titrations involved 19 injections of 2 μL at 180 s intervals. The syringe stirring speed was set at 1000 rpm. Reference titrations of ligands into buffer were used to correct for heats of dilution. All ITC measurements were carried out at 298 K in 20 mM HEPES buffer at pH 8. The thermodynamic data were processed with Origin 7.0 software provided by MicroCal.

Biological methods

Reference compounds, media, and other cell culture reagents were purchased from Sigma–Aldrich (Milan, Italy).

Plasmids. The expression vectors expressing the chimeric receptors containing the yeast Gal4 DNA binding domain fused to the human PPARα or PPARγ ligand binding domain (LBD), and the reporter plasmid for these Gal4 chimeric receptors (pGal5TKpGL3) containing five repeats of the Gal4 response elements upstream of a minimal thymidine kinase promoter that is adjacent to the luciferase gene were described previously.[59]

Cell culture and transfections. Human hepatoblastoma cell line HepG2 (Interlab Cell Line Collection, Genoa, Italy) was cultured in minimum essential medium (MEM) containing 10% heat-inactivated fetal bovine serum, penicillin G (100 U mL^{-1}), and streptomycin sulfate (100 μg mL^{-1}) at 37 °C in a humidified atmosphere of 5% CO_2. For transactivation assays, 10^5 cells per well were seeded in a 24-well plate and transfections were performed after 24 h with CAPHOS, a calcium-phosphate method, according to the manufacturer's guidelines. Cells were transfected with expression plasmids encoding the fusion protein Gal4–PPARα LBD or Gal4–PPARγ LBD (30 ng), pGal5TKpGL3 (100 ng), pCMVβgal (250 ng). Four hours after transfection, cells were treated for 20 h with the indicated ligands in triplicate. Luciferase activity in cell extracts was then determined by a luminometer (VICTOR^3 V Multilabel Plate Reader, PerkinElmer). β-Galactosidase activity was determined using *ortho*-nitrophenyl-β-D-galactopyranoside as described previously.[60] All transfection experiments were repeated at least twice.

Real-time PCR. HepG2 cells were incubated for 24 h with Wy 14,643 (50 μM), (*R*)-**2** (50 μM), or (*S*)-**2** (50 μM), starting 24 h after having been depleted of serum. Total RNA was extracted from 1×10^6 cells; reverse transcription and real-time PCR were performed as previously reported.[61,62] Assays-on-demand for human CPT1, CAC, and human actin (cat. nos. Hs00912671m1, Hs01088810g1, and Hs00357333g1, respectively) were purchased from Applied Biosystems. All transcript levels were normalized against the β-actin expression levels.

Western blot analysis. HepG2 cells were incubated for 48 h with Wy 14,643 (50 μM), (*R*)-**2** (50 μM), or (*S*)-**2** (50 μM), starting 24 h after having been depleted of serum. Proteins were electroblotted onto nitrocellulose membranes (Bio-Rad) and subsequently treated with anti-CPT1 (ARP44796_P050, Aviva Systems Biology), anti-CAC,[47] and anti-β-actin (sc-58619, Santa Cruz) antibodies. The immunoreaction was detected by the ECL plus system (Amersham).

Electrophysiological recordings of resting membrane ionic conductances and excitability parameters. All experiments were performed in accordance with the Italian Guidelines for the use of laboratory animals, which conform with the European Community Directive published in 1986 (86/609/EEC). The electrophysiological recordings were done in vitro on the extensor digitorum longus (EDL) muscle dissected from adult male Wistar rats (Charles River Laboratories, Calco, Italy) under urethane anesthesia (1.2 g kg^{-1} i.p.). Soon after the dissection, rats still anaesthetized were euthanized with a urethane overdose. The EDL muscles were immediately placed in a 25 mL bath chamber, maintained at 30 °C, and perfused with normal or chloride-free physiological solution (gassed with 95% O_2 and 5% CO_2; pH 7.2–7.3).[51] The normal (chloride containing) physiological solution had the following composition: 148 mM NaCl, 4.5 mM KCl, 2 mM $CaCl_2$, 1 mM $MgCl_2$, 12 mM $NaHCO_3$, 0.44 mM NaH_2PO_4, 5.5 mM glucose. The chloride-free solution was made by equimolar substitution of methylsulfate salts for NaCl and KCl and nitrate salts for $CaCl_2$ and $MgCl_2$. Using the two intracellular microelectrodes technique, in current clamp mode, the membrane resistance (Rm) and the fiber diameter were calculated. These parameters were obtained by injecting a hyperpolarizing constant square-wave current pulse (100 ms duration) into the muscle fiber through the current electrode and by recording the resulting voltage deflection with a second microelectrode inserted at two distances from the current electrode. The current pulse generation, the acquisition of the voltage records and the calculation of the

fiber constants were done in real time under computer control as described elsewhere.[51] The reciprocal of Rm from each fiber in normal physiological solution was the total membrane conductance (gm), and the same parameter measured in chloride-free solution was the potassium conductance (gK). The mean chloride conductance (gCl) was estimated as the mean gm minus the mean gK value. The tested compounds were dissolved in DMSO and applied in vitro on muscle bath. Resting gm and gK were measured before and 30 min after addition of increasing concentrations of each compound. The maximal concentration of DMSO used (0.5%) was without effect on the parameters studied.

The excitability parameters of sampled fibers were determined by recording the intracellular membrane potential response to square-wave depolarizing constant current pulses. In each fiber the membrane potential was set by a steady holding current to −80 mV, before passing the depolarizing pulse. The current intensity was gradually increased until the depolarization was just sufficient to elicit a single action potential, and then further increased to generate two or more action potentials. In this way, it was possible to record and measure these parameters: the minimum current intensity that would elicit a single action potential (Ith), the membrane potential at which a single action potential could be elicited (Th), the amplitude of action potential (AP), the latency, that is, the maximal delay from the beginning of the current pulse to the onset of the spike (Lat) and the maximum number of action potentials that the muscle fibers could generate (*N* spikes).

Calcium microspectrofluorimetric analysis. Calcium fluorescence measurements were performed on tendon-to-tendon isolated EDL muscle fibers using a QuantiCell 900 integrated imaging system (VisiTech International Ltd., Sunderland, UK) as previously described.[63] Fura-2-loaded muscle fibers were mounted in a modified glass-bottomed RC-27NE experimental chamber (Warner Instrument Corp., Hamden, USA), setting the sarcomere length at 2.4–2.5 μm, and then placed on the stage of an inverted Eclipse TE300 microscope with a 40× Plan-Fluor objective (Nikon, Japan). Pairs of background-subtracted images of the fura-2 fluorescence (510 nm) excited at 340 and 380 nm were acquired at rest, and pixel-to-pixel ratiometric images were calculated for each muscle fiber. Resting ratio values were used to monitor cytosolic calcium level.

Glossary

PPAR: peroxisome proliferator-activated receptor; LBD: ligand binding domain; TZDs: thiazolidinediones; CAC: carnitine/acylcarnitine carrier; CPT1: carnitine palmitoyltransferase 1; ITC: isothermal titration calorimetry; CDK5: cyclin-dependent kinase 5; ClC-1: chloride channel 1.

Acknowledgements

This work was accomplished thanks to financial support from the Cariplo Foundation (file 2009-2727) and the Ministero dell'Istruzione, dell'Università e della Ricerca [MIUR 2009K7R7NA (F.L.), MIUR 2010W7YRLZ_003 (A.L.)].

Keywords: X-ray crystallography · molecular recognition · PPAR modulators · receptors

[1] J. P. Berger, T. E. Akiyama, P. T. Meinke, *Trends Pharmacol. Sci.* **2005**, *26*, 244–251.

[2] J. Berger, D. E. Moller, *Annu. Rev. Med.* **2002**, *53*, 409–435.

[3] S. A. Kliewer, S. S. Sundseth, S. A. Jones, P. J. Brown, G. B. Wisely, C. S. Koble, P. Devchand, W. Wahli, T. M. Willson, J. M. Lenhard, J. M. Lehmann, *Proc. Natl. Acad. Sci. USA* **1997**, *94*, 4318–4323.

[4] R. T. Nolte, G. B. Wisely, S. Westin, J. E. Cobb, M. H. Lambert, R. Kurokawa, M. G. Rosenfeld, T. M. Willson, C. K. Glass, M. V. Milburn, *Nature* **1998**, *395*, 137–143.

[5] R. T. Gampe, Jr., V. G. Montana, M. H. Lambert, A. B. Miller, R. K. Bledsoe, M. V. Milburn, S. A. Kliewer, T. M. Willson, H. E. Xu, *Mol. Cell* **2000**, *5*, 545–555.

[6] T. M. Willson, P. J. Brown, D. D. Sternbach, B. R. Henke, *J. Med. Chem.* **2000**, *43*, 527–550.

[7] A Unified Nomenclature System for the Nuclear Receptor Superfamily: Nuclear Receptors Nomenclature Committee, *Cell* **1999**, *97*, 161–163.

[8] J. Berger, P. Bailey, C. Biswas, C. A. Cullinan, T. W. Doebber, N. S. Hayes, R. Saperstein, R. G. Smith, M. D. Leibowitz, *Endocrinology* **1996**, *137*, 4189–4195.

[9] N. D. Oakes, C. J. Kennedy, A. B. Jenkins, D. R. Laybutt, D. J. Chisholm, E. W. Kraegen, *Diabetes* **1994**, *43*, 1203–1210.

[10] R. W. Nesto, D. Bell, R. O. Bonow, V. Fonseca, S. M. Grundy, E. S. Horton, M. L. Le Winter, D. Porte, C. F. Semenkovich, S. Smith, L. H. Young, R. Kahn, *Diabetes Care* **2004**, *27*, 256–263.

[11] S. E. Kahn, B. Zinman, J. M. Lachin, S. M. Haffner, W. H. Herman, R. R. Holman, B. G. Kravitz, D. Yu, M. A. Heise, R. P. Aftring, G. Viberti, *Diabetes Care* **2008**, *31*, 845–851.

[12] S. Rocchi, F. Picard, J. Vamecq, L. Gelman, N. Potier, D. Zeyer, L. Dubuquoy, P. Bac, M. F. Champy, K. D. Plunket, L. M. Leesnitzer, S. G. Blanchard, P. Desreumaux, D. Moras, J. P. Renaud, J. Auwerx, *Mol. Cell* **2001**, *8*, 737–747.

[13] J. P. Berger, A. E. Petro, K. L. Macnaul, L. J. Kelly, B. B. Zhang, K. Richards, A. Elbrecht, B. A. Johnson, G. Zhou, T. W. Doebber, C. Biswas, M. Parikh, N. Sharma, M. R. Tanen, G. M. Thompson, J. Ventre, A. D. Adams, R. Mosley, R. S. Surwit, D. E. Moller, *Mol. Endocrinol.* **2003**, *17*, 662–676.

[14] P. Misra, R. Chakrabarti, R. K. Vikramadithyan, G. Bolusu, S. Juluri, J. Hiriyan, C. Gershome, A. Rajjak, P. Kashireddy, S. Yu, S. Surapureddi, C. Qi, Y.-J. Zhu, M. S. Rao, J. K. Reddy, R. Ramanujam, *J. Pharmacol. Exp. Ther.* **2003**, *306*, 763–771.

[15] H. Minoura, S. Takeshita, M. Ita, J. Hirosumi, M. Mabuchi, I. Kawamura, S. Nakajima, O. Nakayama, H. Kayakiri, T. Oku, A. Ohkubo-Suzuki, M. Fukagawa, H. Kojo, K. Hanioka, N. Yamasaki, T. Imoto, Y. Kobayashi, S. Mutoh, *Eur. J. Pharmacol.* **2004**, *494*, 273–281.

[16] J. J. Acton III, R. M. Black, A. B. Jones, D. E. Moller, L. Colwell, T. W. Doebber, K. L. MacNaul, J. Berger, H. B. Wood, *Bioorg. Med. Chem. Lett.* **2005**, *15*, 357–362.

[17] J. F. Dropinski, T. Akiyama, M. Einstein, B. Habulihaz, T. Doebber, J. P. Berger, P. T. Meinke, G. Q. Shi, *Bioorg. Med. Chem. Lett.* **2005**, *15*, 5035–5038.

[18] A. Reifel-Miller, K. Otto, E. Hawkins, R. Barr, W. R. Bensch, C. Bull, S. Dana, K. Klausing, J.-A. Martín, R. Rafaeloff-Phail, C. Rafizadeh-Montrose, G. Rhodes, R. Robey, I. Rojo, D. Rungta, D. Snyder, K. Wilbur, T. Zhang, R. Zink, A. Warshawsky, J. T. Brozinick, *Mol. Endocrinol.* **2005**, *19*, 1593–1605.

[19] J. A. Martín, D. A. Brooks, L. Prieto, R. González, A. Torrado, I. Rojo, B. López de Uralde, C. Lamas, R. Ferritto, M. D. Martín-Ortega, J. Agejas, F. Parra, J. R. Rizzo, G. A. Rhodes, R. L. Robey, C. A. Alt, S. R. Wendel, T. Y. Zhang, A. Reifel-Miller, C. Montrose-Rafizadeh, J. T. Brozinick, E. Hawkins, E. A. Misener, D. A. Briere, R. Ardecky, J. D. Fraser, A. M. Warshawsky, *Bioorg. Med. Chem. Lett.* **2005**, *15*, 51–55.

[20] E. Burgermeister, A. Schnoebelen, A. Flament, J. Benz, M. Stihle, B. Gsell, A. Rufer, A. Ruf, B. Kuhn, H. P. Märki, J. Mizrahi, E. Sebokova, E. Niesor, M. Meyer, *Mol. Endocrinol.* **2006**, *20*, 809–830.

[21] T. Allen, F. Zhang, S. A. Moodie, L. E. Clemens, A. Smith, F. Gregoire, A. Bell, G. E. Muscat, T. A. Gustafson, *Diabetes* **2006**, *55*, 2523–2533.

[22] M. C. Carmona, K. Louche, B. Lefebvre, A. Pilon, N. Hennuyer, V. Audinot-Bouchez, C. Fievet, G. Torpier, P. Formstecher, P. Renard, P. Lefebvre, C. Dacquet, B. Staels, L. Casteilla, L. Pénicaud, Consortium of the French Ministry of Research and Technology, *Diabetes* **2007**, *56*, 2797–2808.

[23] M. K. Kim, Y. N. Chae, H. S. Kim, S.-h. Choi, M. H. Son, S. H. Kim, J. K. Kim, H. S. Moon, S. K. Park, Y. A. Shin, J. G. Kim, C. H. Lee, J. I. Lim, C. Y. Shin, *Arch. Pharmacal Res.* **2009**, *32*, 721–727.

[24] A. Motani, Z. Wang, J. Weiszmann, L. R. McGee, G. Lee, Q. Liu, J. Staunton, Z. Fang, H. Fuentes, M. Lindstrom, J. Liu, D. H. Biermann, J. Jaen, N. P. Walker, R. M. Learned, J. L. Chen, Y. Li, *J. Mol. Biol.* **2009**, *386*, 1301 – 1311.
[25] F. M. Gregoire, F. Zhang, H. J. Clarke, T. A. Gustafson, D. D. Sears, S. Favelyukis, J. Lenhard, D. Rentzeperis, L. E. Clemens, Y. Mu, B. E. Lavan, *Mol. Endocrinol.* **2009**, *23*, 975 – 988.
[26] W. S. Aronow, P. R. Harding, M. Khursheed, J. S. Vangrow, N. P. Papageorge's, J. Mays, *Clin. Pharmacol. Ther.* **1973**, *14*, 358 – 365.
[27] W. S. Aronow, P. R. Harding, M. Khursheed, J. S. Vangrow, N. P. Papageorge's, *Clin. Pharmacol. Ther.* **1973**, *14*, 371 – 373.
[28] T. Rauch, B. S. Hamilton, M. Tsutsumi (Boehringer Ingelheim International GmbH), Int. PCT Pub. No. WO 2013167554 A1 20131114, **2013**.
[29] B. S. Hamilton, T. Rauch, M. Tsutsumi (Boehringer Ingelheim International GmbH), Int. PCT Pub. No. WO 2012059416 A1 20120510, **2012**.
[30] A. Chandalia, H. J. Clarke, L. E. Clemens, B. Pandey, V. Vicena, P. Lee, B. E. Lavan, F. M. Gregoire, *PPAR Res.* **2009**, 706852.
[31] K. L. Luskey, J. Luo (Metabolex Inc., Hayward, USA), US Pat. No. 6.262.118 B1, **2001**.
[32] Y. Zhu, P. Cheng, X. Chen, J. Ma, Z. Zhao (Metabolex Inc., Hayward, USA), US Pat. No. 2007/0072858 A1, **2007**.
[33] D. R. Feller, V. S. Kamanna, H. A. Newman, K. J. Romstedt, D. T. Witiak, G. Bettoni, S. H. Bryant, D. Conte-Camerino, F. Loiodice, V. Tortorella, *J. Med. Chem.* **1987**, *30*, 1265 – 1267.
[34] G. Bettoni, F. Loiodice, V. Tortorella, D. Conte-Camerino, M. Mambrini, E. Ferrannini, S. H. Bryant, *J. Med. Chem.* **1987**, *30*, 1267 – 1270.
[35] C. Hodel, *Toxicol. Lett.* **2002**, *128*, 159 – 168.
[36] S. Pierno, M. P. Didonna, V. Cippone, A. De Luca, M. Pisoni, A. Frigeri, G. P. Nicchia, M. Svelto, G. Chiesa, C. Sirtori, E. Scanziani, C. Rizzo, D. De Vito, D. Conte Camerino, *Br. J. Pharmacol.* **2006**, *149*, 909 – 919.
[37] P. Cheng, J. Ma, X. Chen, Y. Zhu, Z. Zhao (Metabolex Inc., Hayward, USA), Int. PCT Pub. No. WO 2007/038277 A2, **2007**.
[38] M. Wolter, G. Nordmann, G. E. Job, S. L. Buchwald, *Org. Lett.* **2002**, *4*, 973 – 976.
[39] M. M. Cavalluzzi, C. Bruno, G. Lentini, A. Lovece, A. Catalano, A. Carocci, C. Franchini, *Tetrahedron: Asymmetry* **2009**, *20*, 1984 – 1991.
[40] Q. He, Y.-F. Peng, S. Rohani, *Chirality* **2010**, *22*, 16 – 23.
[41] A. Pinelli, C. Godio, A. Laghezza, N. Mitro, G. Fracchiolla, V. Tortorella, A. Lavecchia, E. Novellino, J.-C. Fruchart, B. Staels, M. Crestani, F. Loiodice, *J. Med. Chem.* **2005**, *48*, 5509 – 5519.
[42] A. Laghezza, G. Pochetti, A. Lavecchia, G. Fracchiolla, S. Faliti, L. Piemontese, C. Di Giovanni, V. Iacobazzi, V. Infantino, R. Montanari, D. Capelli, P. Tortorella, F. Loiodice, *J. Med. Chem.* **2013**, *56*, 60 – 72.
[43] C. Temporini, G. Pochetti, G. Fracchiolla, L. Piemontese, R. Montanari, R. Moaddel, A. Laghezza, F. Altieri, L. Cervoni, D. Ubiali, E. Prada, F. Loiodice, G. Massolini, E. Calleri, *J. Chromatogr. A* **2013**, *1284*, 36 – 43.
[44] L. Porcelli, F. Gilardi, A. Laghezza, L. Piemontese, N. Mitro, A. Azzariti, F. Altieri, L. Cervoni, G. Fracchiolla, M. Giudici, U. Guerrini, A. Lavecchia, R. Montanari, C. Di Giovanni, A. Paradiso, G. Pochetti, G. M. Simone, P. Tortorella, M. Crestani, F. Loiodice, *J. Med. Chem.* **2012**, *55*, 37 – 54.
[45] E. Calleri, G. Fracchiolla, R. Montanari, G. Pochetti, A. Lavecchia, F. Loiodice, A. Laghezza, L. Piemontese, G. Massolini, C. Temporini, *J. Chromatogr. A* **2012**, *1232*, 84 – 92.
[46] S. M. Rangwala, M. L. O'Brien, V. Tortorella, A. Longo, F. Loiodice, D. J. Noonan, D. R. Feller, *Chirality* **1997**, *9*, 37 – 47.
[47] V. Iacobazzi, P. Convertini, V. Infantino, P. Scarcia, S. Todisco, F. Palmieri, *Biochem. Biophys. Res. Commun.* **2009**, *388*, 643 – 647.
[48] C. Indiveri, V. Iacobazzi, A. Tonazzi, N. Giangregorio, V. Infantino, P. Convertini, L. Console, F. Palmieri, *Mol. Aspects Med.* **2011**, *32*, 223 – 233.
[49] R. A. Laskowski, M. B. Swindells, *J. Chem. Inf. Model.* **2011**, *51*, 2778 – 2786.
[50] J. H. Choi, A. S. Banks, J. L. Estall, S. Kajimura, P. Boström, D. Laznik, J. L. Ruas, M. J. Chalmers, T. M. Kamenecka, M. Blüher, P. R. Griffin, B. M. Spiegelman, *Nature* **2010**, *466*, 451 – 456.
[51] S. Pierno, G. M. Camerino, V. Cippone, J.-F. Rolland, J.-F. Desaphy, A. De Luca, A. Liantonio, G. Bianco, J. D. Kunic, A. L. George, Jr., D. Conte Camerino, *Br. J. Pharmacol.* **2009**, *156*, 1206 – 1215.
[52] G. Fracchiolla, A. Laghezza, L. Piemontese, P. Tortorella, F. Mazza, R. Montanari, G. Pochetti, A. Lavecchia, E. Novellino, S. Pierno, D. Conte Camerino, F. Loiodice, *J. Med. Chem.* **2009**, *52*, 6382 – 6393.
[53] M. W. Berchtold, H. Brinkmeier, M. Müntener, *Physiol. Rev.* **2000**, *80*, 1215 – 1265.
[54] S. Pierno, J. F. Desaphy, A. Liantonio, A. De Luca, A. Zarrilli, L. Mastrofrancesco, G. Procino, G. Valenti, D. Conte Camerino, *J. Physiol.* **2007**, *584*, 983 – 995.
[55] G. Pochetti, C. Godio, N. Mitro, D. Caruso, A. Galmozzi, S. Scurati, F. Loiodice, G. Fracchiolla, P. Tortorella, A. Laghezza, A. Lavecchia, E. Novellino, F. Mazza, M. Crestani, *J. Biol. Chem.* **2007**, *282*, 17314 – 17324.
[56] A. G. W. Leslie, *Newsl. Protein Crystallogr.* **1992**, *26*, 27 – 33.
[57] J. Navaza, *Acta Crystallogr. Sect. A* **1994**, *50*, 157 – 163.
[58] P. D. Adams, P. V. Afonine, G. Bunkóczi, V. B. Chen, I. W. Davis, N. Echols, J. J. Headd, L.-W. Hung, G. J. Kapral, R. W. Grosse-Kunstleve, A. J. McCoy, N. W. Moriarty, R. Oeffner, R. J. Read, D. C. Richardson, J. S. Richardson, T. C. Terwilliger, P. H. Zwart, *Acta Crystallogr. Sect. D* **2010**, *66*, 213 – 221.
[59] E. Raspé, L. Madsen, A. M. Lefebvre, I. Leitersdorf, L. Gelman, J. Peinado-Onsurbe, J. Dallongeville, J.-C. Fruchart, R. Berge, B. Staels, *J. Lipid Res.* **1999**, *40*, 2099 – 2110.
[60] T. Hollon, F. K. Yoshimura, *Anal. Biochem.* **1989**, *182*, 411 – 418.
[61] V. Iacobazzi, V. Infantino, P. Convertini, A. Vozza, G. Agrimi, F. Palmieri, *Biochem. Biophys. Res. Commun.* **2009**, *386*, 186 – 191.
[62] P. Convertini, V. Infantino, F. Bisaccia, F. Palmieri, V. Iacobazzi, *Biochem. Biophys. Res. Commun.* **2011**, *404*, 376 – 381.
[63] B. Fraysse, J. F. Desaphy, S. Pierno, A. De Luca, A. Liantonio, C. I. Mitolo, D. Conte Camerino, *FASEB J.* **2003**, *17*, 1916 – 1918.

Received: October 24, 2014Published online on ■■ ▮▮, 0000

*A. Laghezza, R. Montanari, A. Lavecchia, L. Piemontese, G. Pochetti, V. Iacobazzi, V. Infantino, D. Capelli, M. De Bellis, A. Liantonio, S. Pierno, P. Tortorella, D. Conte Camerino, F. Loiodice**

■■ – ■■

On the Metabolically Active Form of Metaglidasen: Improved Synthesis and Investigation of Its Peculiar Activity on Peroxisome Proliferator-Activated Receptors and Skeletal Muscles

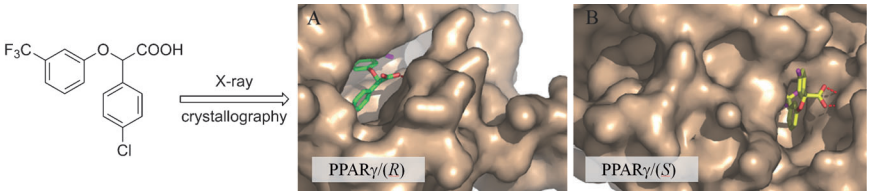

Unexpected activity: The metabolically active forms of the selective PPARγ modulator metaglidasen and its enantiomer were carefully investigated toward PPARα. Unexpectedly, the former showed antagonist activity, whereas the latter behaved as a partial agonist. Crystallographic studies on PPARγ were performed to gain more insight on molecular-level interactions. Both stereoisomers also showed blocking activity on skeletal muscle chloride conductance.